The Journal of Physical Chemistry

 VOLUME 100, NUMBER 50, DECEMBER 12, 1996

LETTERS

Photoelectron Spectroscopy and Electronic Structure of Met-Car Ti_8C_{12}

Lai-Sheng Wang,* San Li, and Hongbin Wu

Department of Physics, Washington State University, Richland, Washington 99352, and Environmental Molecular Sciences Laboratory, Pacific Northwest National Laboratory, MS K2-14, P.O. Box 999, Richland, Washington 99352

Received: October 7, 1996[⊗]

Photoelectron spectroscopy experiments are performed on a metallocarbohedrene, $Ti_8C_{12}^-$, to obtain electronic structure information. The $Ti_8C_{12}^-$ anion is produced by laser vaporization of a titanium carbide target. The spectra of $Ti_8C_{12}^-$ consist of an intense threshold feature and two weaker features followed by a gap and more higher energy features. The electron affinity of Ti_8C_{12} is found to be 1.05 (±0.05) (adiabatic) and 1.16 (±0.05) eV (vertical). The surprisingly low electron affinity and the observed electronic features are interpreted using theoretical electronic structure information. The current experiments provide hitherto the most direct spectroscopic information on the Met-Car Ti_8C_{12}.

The discovery of the metallocarbohedrenes (Met-Cars) by Castleman and co-workers[1] represents a significant development in cluster science following the discovery and subsequent bulk synthesis of fullerenes.[2] The Met-Cars (M_8C_{12}) consisting of 8 early transition metal atoms and 12 carbon atoms are expected to exhibit even richer chemical and physical properties that may find applications in electronics, catalysis, and magnetic materials. The original discovery has been followed by intensive theoretical[3−7] and experimental works.[8−14] However, its structure is still the center of much contention. In particular, the lack of direct spectroscopic information makes it difficult to verify the various theoretical calculations.

Castleman *et al*. initially proposed a dodecahedral structure (T_h) for the Met-Cars.[1] Chemical reaction studies are used to support this structure.[9,10] It can be viewed as a cubic M_8 cluster with six C_2 units capping the six faces of the cube.[3] Theoretical considerations predict that Ti_8C_{12} with T_h symmetry will undergo Jahn−Teller distortion.[4] Several calculations have suggested lower symmetry structures with much lower energies.[4−7] The most stable one is a tetrahedral cluster (T_d), which has received the most theoretical attention recently.[5−7] It involves distorting the M_8 cube into a tetracapped tetrahedral M_8 cluster with the six C_2 units along the six edges of the outer tetrahedron formed by the four capping M atoms. Ion chromatography (IC) experiments suggest that the T_h Met-Car ($Ti_8C_{12}^+$) fits the IC data best but cannot exclude the T_d structure within the experimental uncertainty.[14] Recent chemical reaction experiments on $V_8C_{12}^+$ and $Nb_8C_{12}^+$ seem to suggest that they are consistent with the T_d structure.[13]

Theoretically, the T_d structure is vastly more stable than the T_h structure by as much as 300 kcal/mol.[5−7] Recently it has been shown that the transformation from the T_h to T_d structure is barrierless.[7] Extensive theoretical efforts have been made on the T_d structure with explicit predictions for its electronic structure.[6] In principle, experimental electronic structure information can be used to test these predictions. Unfortunately, there are scarce experimental electronic structure information and few quantitative experimental data to test the different calculations. Chemical reaction studies of $Ti_8C_{12}^+$ with halogen hydrocarbons found that $Ti_8C_{12}^+$ is able to abstract one halogen atom to form $Ti_8C_{12}(L)^+$ (L = Cl, I), suggesting that $Ti_8C_{12}^+$ has one unpaired electron that can be donated to the halogen

[⊗] Abstract published in *Advance ACS Abstracts,* December 1, 1996.

S0022-3654(96)03068-7 CCC: $12.00

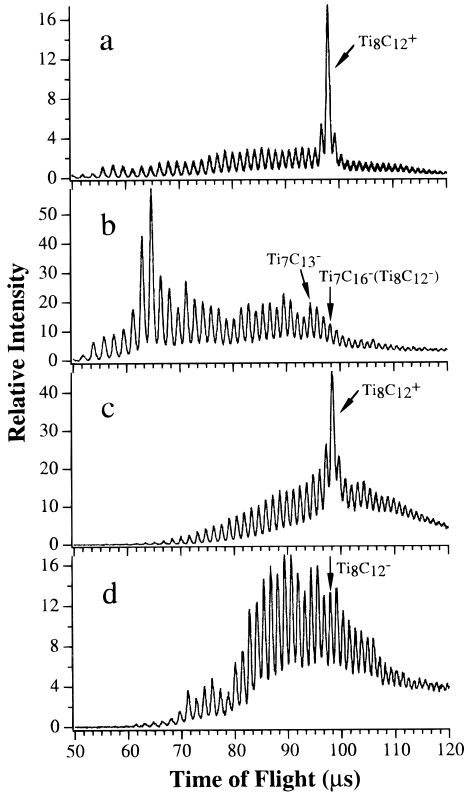

Figure 1. (a) Positive ion mass spectrum of $Ti_xC_y^+$ clusters when a titanium target is vaporized with a 5% CH_4 seeded helium carrier gas, showing the "magic" $Ti_8C_{12}^+$ Met-Car. Laser vaporization conditions: 10 mJ/pulse at 532 nm, 7 ns pulse width. (b) Negative ion mass spectrum of $Ti_xC_y^-$ clusters under similar conditions as (a), showing that the anticipated Met-Car anion $Ti_8C_{12}^-$ is not produced (see text). (c) Positive ion mass spectrum of $Ti_xC_y^+$ clusters when a solid TiC target is vaporized with neat helium carrier gas, showing the "magic" $Ti_8C_{12}^+$ Met-Car. Laser vaporization conditions: 3 mJ/pulse at 532 nm, 7 ns pulse width. (d) Negative ion mass spectrum of $Ti_xC_y^-$ clusters under similar conditions as (c) (7 mJ/pulse), showing that the Met-Car anion $Ti_8C_{12}^-$ is produced with significant abundance (see refs 16 and 18).

atom.[10] Recent experiments on the ionization potentials (IP) of the Met-Cars find an anomalously low IP for Ti_8C_{12} (4.9 ± 0.2 eV).[12] Photoelectron spectroscopy (PES) of size-selected anions has been a powerful technique to probe the electronic structure of metal clusters.[15] Here we present the first PES study on the Met-Car $Ti_8C_{12}^-$, providing direct electronic structure information.

The apparatus used in this work has been described in detail previously.[15] The key in the current experiment is how to produce the Met-Car $Ti_8C_{12}^-$ anion. The Met-Car cation ($Ti_8C_{12}^+$) was originally discovered by laser vaporization of pure titanium with a hydrocarbon seeded helium carrier gas.[1a] The plasma reactions between the laser-vaporized titanium atomic species and the hydrocarbons produce the magic Met-Car *cations*. Figure 1a shows one such mass spectrum for $Ti_8C_{12}^+$ when a Ti target is vaporized (10 mJ/pulse, 532 nm) with a helium carrier gas containing 5% CH_4. However, the negative ion spectrum (Figure 1b) under similar conditions is completely different. Various intense small $Ti_xC_y^-$ clusters are observed, while the $Ti_8C_{12}^-$ peak is totally nonmagic. Due to the mass coincidence between one Ti and four C, the carbon-13 isotope is required to assign the mass pattern to definitive $Ti_xC_y^-$ clusters. Upon such isotope experiments with $^{13}CH_4$, we find that the peak expected for $Ti_8C_{12}^-$ is actually $Ti_7C_{16}^-$ (Figure 1b). The spectrum shown in Figure 1b in fact contains almost no $Ti_8C_y^-$ species.

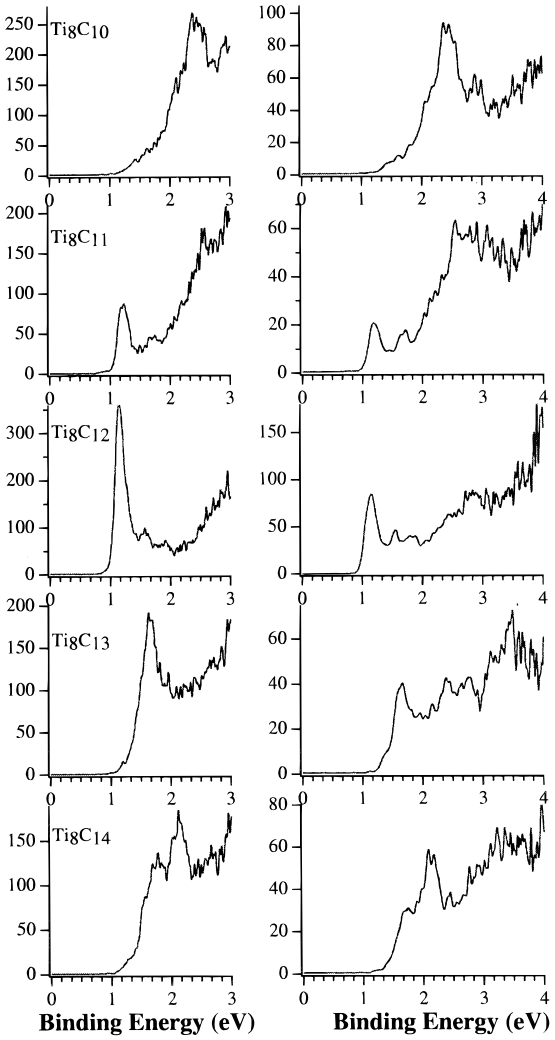

Figure 2. Photoelectron spectra of $Ti_8C_y^-$ ($y = 10-14$) at two detachment laser energies: left panel, 3.49 eV (355 nm); right panel, 4.66 eV (266 nm). Note the special nature of the $Ti_8C_{12}^-$ spectra.

The $Ti_8C_{12}^-$ clusters are produced by laser vaporization of a solid TiC target with neat helium carrier gas. Figure 1c shows a positive mass spectrum when only 3 mJ/pulse vaporization power is used. We find that the TiC target yields more abundant $Ti_xC_y^+$ clusters and the magic $Ti_8C_{12}^+$ is easily made. Higher vaporization power is required in the pure Ti/CH_4 case to produce an intense plasma for the dehydrogenation reactions necessary to produce the Ti_xC_y clusters. Figure 1d shows the negative ion mass spectrum with the TiC target under similar conditions as in Figure 1c. It is quite different from Figure 1b. Even though here the $Ti_8C_{12}^-$ cluster is still not magic, it is produced with significant abundance.[16] We will show below that the low abundance of $Ti_8C_{12}^-$ is due to the unusually low electron affinity of Ti_8C_{12}.

With the TiC target, the $Ti_xC_y^-$ cluster anions are produced at every 12 amu starting from TiC_4^-.[16] We have obtained PES spectra for all the mass channels starting from TiC_4^- up to $Ti_9C_y^-$.[17] Figure 2 displays the spectra of $Ti_8C_y^-$ ($y = 10-14$) taken at two different photon energies, 3.49 and 4.66 eV.[18] The $Ti_8C_{12}^-$ spectrum is quite special with an intense threshold peak, from which we obtain the electron affinity (EA) of Ti_8C_{12}, 1.05 (±0.05) (adiabatic) and 1.16 (±0.05) eV (vertical). The Ti_8C_{12} cluster has the lowest EA among the species shown in Figure 2. In fact, it is among the lowest EA species of all the Ti_xC_y clusters that we have measured from TiC_4 up to Ti_9C_y.[17] This anomalously low EA for Ti_8C_{12} is at least partially responsible for the low mass abundance of $Ti_8C_{12}^-$ (Figure 1d). The PES

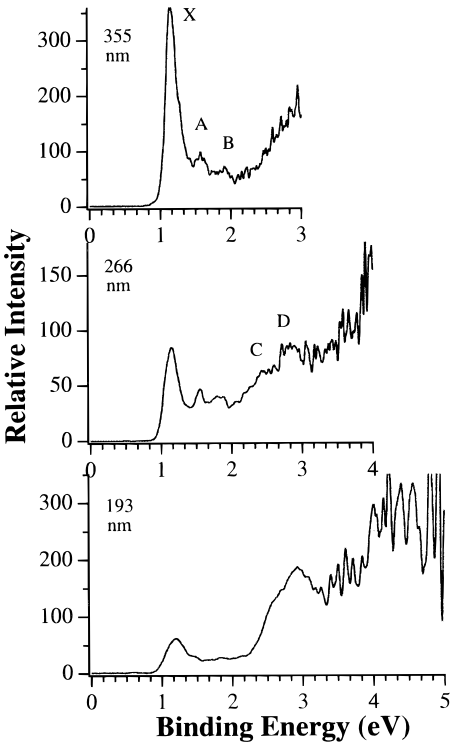

Figure 3. Comparison of the photoelectron spectra of $Ti_8C_{12}^-$ at three photon energies: top, 355 nm (3.49 eV); middle, 266 nm (4.66 eV); bottom, 193 nm (6.42 eV).

spectra of $Ti_8C_{11}^-$ and $Ti_8C_{13}^-$ are also somewhat special (Figure 2). We think that this is related to the special character of these two clusters that also shows up in the positive ion mass spectra: $Ti_8C_{11}^+$ and $Ti_8C_{13}^+$ always accompany the magic $Ti_8C_{12}^+$ peak with higher abundance than other neighboring $Ti_xC_y^+$ clusters (Figure 1a,c). IC experiments find that the cations of all three clusters ($Ti_8C_{12}^+$, $Ti_8C_{11}^+$, and $Ti_8C_{13}^+$) show similar mobilities, i.e., similar shapes.[14] We focus on the $Ti_8C_{12}^-$ PES spectra presently.

The PES spectra of $Ti_8C_{12}^-$ at three different photon energies are compared in Figure 3. At 3.49 eV, three features are clearly observed, X (1.16 eV), A (~1.56 eV), and B (~1.81 eV). Signals at higher binding energies are also observed. These are shown more clearly at the higher photon energy spectra, labeled as C (~2.5 eV) and D (~2.9 eV). More transitions are shown at the 6.42 eV spectra but are not well resolved due to poor signal-to-noise ratio. The features A and B are barely visible in the 6.42 eV spectrum due to poor resolution and lower signals at this photon energy. It can be seen from the 6.42 eV spectrum that the spectral features may be divided into two groups, the lower energy features (X, A, B) followed by a small energy gap (~0.7 eV) and more transitions at higher BE (C and D).

The anomalous EA and the well-defined spectral features of the $Ti_8C_{12}^-$ spectra suggest that the observed spectra are indeed due to the Met-Car that we are interested in. First, the low EA is consistent with the unusually low IP measured for the Ti_8C_{12} Met-Car.[12] Second, both these observations and the PES spectral features can be interpreted from the theoretical electronic structure calculations based on the T_d structure, which has recently received the most theoretical attention because of its enormous stability compared to other structures.[5−7]

Under the T_d structure, the six C_2 units are end-on bonded to the four outer Ti atoms through σ bonding and side-on bonded to the four inner Ti atoms through π bonding.[5−7] Each C_2 may be viewed as an acetylene-like unit (C_2^{2-}). Each metal atom has three d orbitals for metal−metal interactions that form the valence orbitals of the Met-Car. Figure 4 shows a schematic orbital diagram for these interactions,[6a] where $1a_1$, $1t_2$, 1e, and $1t_1$ are bonding orbitals and $2a_1$, $2t_2$, $3t_2$, 2e, $2t_1$, and $4t_2$ are antibonding orbitals. The filling of the nine bonding orbitals is expected to make an especially stable cluster. Among the 32 valence electrons on the Ti atoms in Ti_8C_{12}, only 20 are available for the metal−metal interactions (12 are donated to the 6 C_2 units). These are two electrons too many to make the stable 18-electron configuration. The two extra electrons fill the higher energy $2a_1$ orbital. This is consistent with the low IP measured for the Ti_8C_{12} Met-Car since the $2a_1$ electrons are expected to be easily ionized. In fact, it has been suggested that the dication $[Ti_8C_{12}]^{2+}$ might be specially stable and may be the best target for synthesis in bulk form.[6a] Figure 4 is also consistent with the halogen abstraction experiments that suggest that the $Ti_8C_{12}^+$ cation has one unpaired electron.[10] Our PES spectra shown in Figure 2 can be understood on the basis of this orbital diagram.

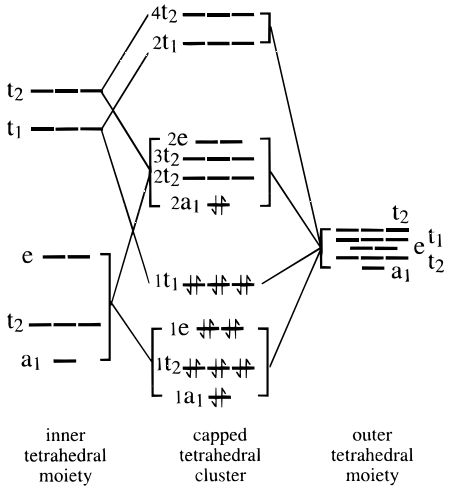

Figure 4. Schematic orbital diagram showing the valence molecular orbitals resulting from the metal−metal interactions for a tetracapped Ti_8C_{12} Met-Car (from ref 6a). It is used to interpret the observed photoelectron spectra of $Ti_8C_{12}^-$. In the anion, $Ti_8C_{12}^-$, the extra electron resides in the $2t_2$ orbital.

In the anion, the extra electron enters the $2t_2$ orbital. Since the $2t_2$ orbital is further up in energy, a low EA for Ti_8C_{12} is easily understandable. The occupation of the $2t_2$ orbital leads to a $^2T_2$ degenerate ground state for $Ti_8C_{12}^-$, which is subject to Jahn−Teller distortion. Within the single-particle picture, the detachment of the electron from the $2t_2$ orbital yields the ground state PES feature (X, Figure 3). The width of this feature suggests that there is a geometry change from the anion to the neutral transition. This may be due to the anticipated Jahn−Teller effect. The removal of a $2a_1$ electron will produce the two low-lying states (A and B, Figure 3) due to the singlet−triplet coupling. The A feature with lower energy is likely to be the singlet state by removing a spin-up $2a_1$ electron, while the B state is the triplet state due to the removal of the spin-down $2a_1$ electron. The A−B energy separation yields a singlet−triplet coupling energy of ~0.25 eV. Following an energy gap of ~0.7 eV, the C and D features are from removal of electrons from the highest occupied bonding orbitals ($1t_1$). Even higher energy features seen in the 6.42 eV spectrum are then due to removal of electrons from other bonding orbitals. The relative intensities of the spectral features support the various orbital characteristics. The A and B features have the lowest intensities because their orbital origin ($2a_1$) is nondegenerate.

Thus the electronic structure of the T_d Ti_8C_{12} is not only consistent with several experimental observations, such as low IP (high cation abundance), chemisorption of only four π-bonding molecules, low EA (lower abundance of anion), and halogen abstraction reactions, but also allows a detailed interpretation of the current PES spectra. These lend considerable credence to the validity of this structure. More accurate *ab initio* calculations that can consistently predict precise IP and EA values in agreement with the experimental measurements should provide the definitive structure for the Met-Cars.

Acknowledgment. The support of this research by the National Science Foundation through a CAREER Program Award (DMR-9622733) is gratefully acknowledged. The work is performed at Pacific Northwest National Laboratory, operated for the U.S. Department of Energy by Battelle under Contract DE-AC06-76RLO 1830.

References and Notes

(1) (a) Guo, B. C.; Kerns, K. P.; Castleman, A. W., Jr. *Science* **1992**, *255*, 1411. (b) Guo, B. C.; Wei, S.; Purnell, J.; Buzza, S.; Castleman, A. W., Jr. *Science* **1992**, *256*, 511. (c) Wei, S.; Guo, B. C.; Purnell, J.; Buzza, S.; Castleman, A. W., Jr. *Science* **1992**, *256*, 818.

(2) Kroto, H.; Heath, J. R.; O'Brien, S. C.; Curl, R. F.; Smalley, R. E. *Nature* **1985**, *318*, 1662. Kratschmer, W.; Lamb, L. D.; Fostiropoulos, K.; Huffman, D. R. *Nature* **1990**, *347*, 354.

(3) Grimes, R. W.; Gale, J. D. *J. Chem. Soc., Chem. Commun*. **1992**, 1222. Rantala, T. T.; Jelski, D. A.; Bowser, J. R.; Xia, X.; George, T. F. *Z. Phys. D* **1992**, *26*, S255. Pauling, L. *Proc. Natl. Acad. Sci. U.S.A.* **1992**, *89*, 8175. Lin, Z.; Hall, M. B. *J. Am. Chem. Soc*. **1992**, *114*, 10054. Reddy, B. V.; Khanna, S. N.; Jena, P. *Science* **1992**, *258*, 640. Methfessel, M.; van Schilfgaarde, M.; Scheffler, M. *Phys. Rev. Lett.* **1993**, *71*, 209. Hay, P. J. *J. Phys. Chem*. **1993**, *97*, 3081. Grimes, R. W.; Gale, J. D. *J. Phys. Chem*. **1993**, *97*, 4616. Khan, A. **1993**, *97*, 10937. Reddy, B. V.; Khanna, S. N. *J. Phys. Chem*. **1994**, *98*, 9446. Khan, A. *J. Phys. Chem*. **1995**, *99*, 4923. Lou, L.; Guo, T.; Nordlander, P.; Smalley, R. E. *J. Chem. Phys*. **1993**, *99*, 5301. Reddy, B. V.; Khanna, S. N. *Chem. Phys. Lett*. **1993**, *209*, 104. Lou, L.; Nordlander, P. *Chem. Phys. Lett*. **1994**, *224*, 439.

(4) Ceulemans, A.; Fowler, P. W. *J. Chem. Soc., Faraday Trans*. **1992**, *88*, 2797. Rohmer, M.; de Vaal, P.; Benard, M. *J. Am. Chem. Soc*. **1992**, *114*, 9696. Chen, H.; Feyereisen, M.; Long, X. P.; Fitzgerald, G. *Phys. Rev. Lett*. **1993**, *71*, 1732.

(5) Dance, D. *J. Chem. Soc., Chem. Commun*. **1992**, 1779. Rohmer, M.; Benard, M.; Henriet, C.; Bo, C.; Poblet, J. *J. Chem. Soc., Chem. Commun*. **1993**, 1182. Dance, I. *J. Am. Chem. Soc*. **1996**, *118*, 2699.

(6) (a) Lin, Z.; Hall, M. B. *J. Am. Chem. Soc*. **1993**, *115*, 11165. (b) Rohmer, M.; Benard, M.; Bo, C.; Poblet, J. *J. Am. Chem. Soc*. **1995**, *117*, 508; *J. Phys. Chem*. **1995**, *99*, 16913.

(7) Dance, I. *J. Am. Chem. Soc*. **1996**, *118*, 6309.

(8) Wei, S.; Guo, B. C.; Purnell, J.; Buzza, S.; Castleman, A. W., Jr. *J. Phys. Chem*. **1992**, *96*, 4166; *J. Phys. Chem*. **1993**, *97*, 9559. Cartier, S. F.; May, B. D.; Toleno, B. J.; Purnell, J.; Wei, S.; Castleman, A. W., Jr. *Chem. Phys. Lett*. **1994**, *220*, 23. May, B. D.; Cartier, S. F.; Castleman, A. W., Jr. *Chem. Phys. Lett*. **1995**, *242*, 265; Wei, S.; Guo, B. C.; Deng, H. T.; Purnell, J.; Buzza, S.; Castleman, A. W., Jr. *J. Am. Chem. Soc*. **1994**, *116*, 4475. Cartier, S. F.; May, B. D.; Castleman, A. W., Jr. *J. Am. Chem. Soc*. **1994**, *116*, 5295. *J. Chem. Phys*. **1994**, *100*, 5384. Kerns, K. P.; Guo, B. C.; Deng, H. T.; Castleman, A. W., Jr. *J. Chem. Phys*. **1994**, *101*, 8529. Cartier, S. F.; May, B. D.; Castleman, A. W., Jr. *J. Chem. Phys*. **1996**, *104*, 3423; *J. Phys. Chem*. **1996**, *100*, 8175.

(9) Guo, B. C.; Kerns, K. P.; Castleman, A. W., Jr. *J. Am. Chem. Soc*. **1993**, *115*, 7415. Kerns, K. P.; Guo, B. C.; Deng, H. T.; Castleman, A. W., Jr. *J. Am. Chem. Soc*. **1995**, *117*, 4026.

(10) Deng, H. T.; Kerns, K. P.; Castleman, A. W., Jr. *J. Am. Chem. Soc*. **1996**, *118*, 446. Deng, H. T.; Guo, B. C.; Kerns, K. P.; Castleman, A. W., Jr. *J. Phys. Chem*. **1994**, *98*, 13373.

(11) Pilgrim, J. S.; Duncan, M. A. *J. Am. Chem. Soc*. **1993**, *115*, 4395, 6958, 9724. Pilgrim, J. S.; Duncan, M. A. *Int. J. Mass Spectrom. Ion Processes* **1994**, *138*, 283. Pilgrim, J. S.; Brock, L. R.; Duncan, M. A. *J. Phys. Chem*. **1995**, *99*, 544.

(12) Brock, L. R.; Duncan, M. A. *J. Phys. Chem*. **1996**, *100*, 5654.

(13) Byun, Y. G.; Lee, S. A.; Freiser, B. S. *J. Phys. Chem*. **1996**, *100*, 14281. Yeh, C. S.; Afzaal, S.; Lee, S. A.; Byun, Y. G.; Freiser, B. S. *J. Am. Chem. Soc*. **1994**, *116*, 8806. Byun, Y. G.; Freiser, B. S. *J. Am. Chem. Soc*. **1996**, *118*, 3681.

(14) Lee, S.; Gotts, N. G.; von Helden, G.; Bowers, M. T. *Science* **1995**, *267*, 999.

(15) Wang, L. S.; Cheng, H.; Fan, J. *J. Chem. Phys*. **1995**, *102*, 9480. Wu, H.; Desai, S. R.; Wang, L. S. *Phys. Rev. Lett*. **1996**, *76*, 212.

(16) The apparent continuous mass distribution is caused by the mass coincidence between one Ti and four C. When a ZrC or CrC target is used, we observe that the cluster distributions are grouped according to a given number of metal atoms. For the CrC case, we observe a slightly magic $Cr_8C_{12}^-$ mass peak along with $Cr_8C_y^-$ (y = 10, 11, 13, 14). The clusters with likely stoichiometry to overlap with $Ti_8C_{12}^-$ are $Ti_7C_{16}^-$ and $Ti_9C_8^-$. From the range of metal−carbon compositions for the $M_xC_y^-$ clusters observed for the Zr or Cr systems, these compositions are unlikely.

(17) Li, L.; Wu, H.; Wang, L. S. Unpublished.

(18) The special nature of the PES spectrum of $Ti_8C_{12}^-$ suggests that it has little or no contamination from other $Ti_xC_y^-$ clusters. Additionally, the $Ti_7C_{16}^-$ cluster produced using Ti/CH_4 gives a very different PES spectrum with much higher electron binding energies.

JP9630683